Combining hazard, exposure and vulnerability data to predict historical United States hurricane losses

Alexander F. Vessey[1 *], Alexander J. Baker[2, 3 *], Vernie Marcellin-Honore[2], and James Michelin[2]

[1]AXA XL, 20 Gracechurch Street, London, United Kingdom
[2]Department of Meteorology, University of Reading, Reading, United Kingdom
[3]National Centre for Atmospheric Science, Reading, United Kingdom

Correspondence to: Alexander F. Vessey (alecvessey@hotmail.co.uk) and Alexander J. Baker (alexander.baker@reading.ac.uk)

Abstract. Hurricanes are among the most destructive natural hazards globally. The widely used Saffir–Simpson scale is an effective public-communication tool, but it is based on a single hazard quantity (wind speed) and has low skill in representing historical economic losses. Accurate risk assessment requires hazard, exposure, and vulnerability information. We present a statistical model to predict losses from North Atlantic hurricanes making landfall in the United States using optimally weighted, normalised-rank quantities describing hazard, exposure, and vulnerability. The model significantly outperforms single-parameter predictions, including landfall wind-speed maxima and central-pressure minima. Root-mean-square error between observed losses and losses predicted from landfall wind speed alone is U.S.$ 35.6 bn, which our model reduces to U.S.$ 7.0 bn. To improve the characterisation of risk, we introduce a loss-based 'Hurricane Predictive Loss Scale' to more directly link hurricane characteristics and landfall to financial impacts. These results demonstrate that integrating exposure and vulnerability data with hazard observations yields skilful estimates of historical hurricane losses, and our approach may help assess how loss from a forecast landfall may rank among historical events. This work is applicable to other cyclone-prone regions and highlights the critical need for open-source exposure and vulnerability data to advance climate risk understanding.

Significance statement. Hurricanes are a destructive natural hazard. Historically, however, their Saffir–Simpson categories and losses are not well correlated. We combined hazard, exposure, and vulnerability data to predict losses from landfalling hurricanes for the United States. Our model significantly reduces errors between predicted and observed losses and is more skilful than hazard-only predictions. Additionally, we developed a novel loss-based hurricane classification scheme to aid risk management.

1 Introduction

Intense tropical cyclones are the most impactful meteorological hazard worldwide (Gallagher Re, 2025; Willis Towers Watson, 2024, AON, 2024). Between 1980 and 2024, global economic losses due to tropical cyclone landfalls totals U.S.$ 2.9 tn (National Oceanographic and Atmospheric Administration, 2024), through extreme wind, storm surge and rainfall. Generally, extreme wind induces building damage (Ibrahim *et al*., 2024) and storm surge and intense rainfall cause fatalities (Rappaport, 2014). Improving our understanding of hurricane risk is essential to mitigating impacts through long-term policies, such as strengthened building codes, and short-term preparedness measures, such as early-warning systems.

Skilful hurricane damage assessments are challenging and uncertain, as the impacted area may be large and building damage highly site-specific. Nonetheless, damage assessment reports over the last century agree that the most financially impactful U.S. hurricanes include the Great Miami Hurricane (1926), Katrina (2005), and Harvey (2017) (Delforge *et al.*, 2025; Grinsted *et al.*, 2019; Muller *et al.*, 2025; National Centers for Environmental Information, 2025; Weinkle *et al.*, 2018). There is also evidence that hurricane-related economic losses have increased over time (Grinsted *et al.*, 2019; Klotzbach *et al.*, 2022b), highlighting the urgency of understanding impacts and losses to enhance disaster preparedness and support mitigation. However, uncertainties in studies of high-impact landfalling events are high compared with basin-wide metrics of cyclone activity (Emanuel, 2011). Additionally, significant uncertainty remains over how hurricane-related impacts will evolve in a warming climate (Knutson *et al*., 2020; Meiler *et al*., 2025), including U.S. landfalls (Jewson, 2023), so understanding the key factors responsible for, and which therefore help predict, losses regionally is critical.

Recent work has demonstrated skilful multi-year predictions of North Atlantic hurricane activity and U.S. hurricane damage, but individual high-damage events, particularly those occurring during periods of generally low activity, are not well predicted (Lockwood *et al.*, 2023). Each hurricane-related loss is the result of a unique combination of meteorological and socioeconomic factors, and quantifying hurricane risk requires an understanding of hazard, exposure and vulnerability (Ward *et al.*, 2020). Hazard quantities describe a hurricane's physical characteristics, including intensity, duration, size, and associated perils such as storm surge and rainfall-induced flooding. Exposure variables capture the location and value of affected assets, including residential, commercial, and industrial buildings within the storm's footprint. Vulnerability metrics reflect assets' susceptibility to damage, influenced by construction materials, design and age. To account for these factors, open-source catastrophe models, such as CLIMADA (Aznar-Siguan & Bresch, 2019), HAZUS (Federal Emergency Management Agency, 2024a) and OASIS LMF (Oasis Loss Modelling Framework, 2025), simulate a hurricane's track and estimate damage based on exposure and vulnerability at the landfall location. However, case-study evidence suggests such models significantly underestimate historical loss estimates for hurricanes (König, 2017) and other storm types, such as European windstorms (Welker *et al*., 2021). For hurricanes, this lack of skill may be due to the representation of hazard footprints (e.g., wind, precipitation and storm surge),

resulting from the insufficient resolution of forecast model data or reliance on a parametric wind field (e.g., Holland *et al*., 2010). More complex, proprietary catastrophe models are typically used by (re-)insurers.

North Atlantic hurricanes are categorised using the Saffir–Simpson Hurricane Wind Scale, which indicates damage potential based on 1-minute near-surface wind speed (Kelman, 2013: NOAA, 2021). This scale is a key tool for public communication of hurricane risk (Cass *et al*., 2023). However, as it is based on a single hazard quantity, it does not predict damage sufficiently skilfully (Bloemendaal *et al.*, 2021). At landfall, central sea-level pressure minima are more strongly correlated with normalised historical hurricane damage than wind-speed maxima (Klotzbach *et al.*, 2020; Klotzbach *et al.*, 2022a), likely due to central pressure being physically related to both hurricane maximum wind speed and size (Chavas *et al.*, 2025). To characterise potential hurricane damage, there are calls to modify the Saffir–Simpson scale (Wehner and Kossin, 2024) and develop multi-hazard and multidisciplinary (i.e., hazard, exposure and vulnerability) equivalents (Tripathy *et al*., 2024), to understand hurricane impacts and how risk may evolve in a warming climate (Ward *et al*., 2020; Camelo and Mayo, 2021, Tripathy *et al*., 2024, Gori *et al*., 2025).

To develop a hurricane classification more closely aligned with observed damage, Bloemendaal *et al.* (2021) devised a 'Tropical Cyclone Severity Scale', which categorises hurricanes by incorporating wind speed, storm surge and accumulated rainfall. Hurricanes ranked by this scale corresponded better with historical losses compared with the Saffir–Simpson scale, but several events were still mis-represented and assigned a low category despite causing significant damage. For example, Hurricane Sandy (2012) resulted in an estimated U.S.$ 70 bn in normalised economic losses, but its classification was only changed from category 1 in the Saffir–Simpson scale to category 2 in the 'Tropical Cyclone Severity Scale' (Bloemendaal *et al.*, 2021). Other studies have attempted to develop skilful multidisciplinary scales (i.e., not only hazard information). Pilkington and Mahmoud (2016) used an artificial neural network model to forecast the economic impact from hurricanes using hazard and exposure data, including landfall location, population affected, wind speed, central pressure, precipitation and storm surge. Baldwin *et al.* (2023) showed the importance of differences in vulnerability between conurbations and rural areas for accurately modelling hurricane risk across the Philippines, stressing the importance of including a vulnerability layer to link a given wind speed to a percentage of exposed assets destroyed. These studies highlight the importance of accounting for multiple risk factors.

Focussing on historical U.S. landfalling hurricanes, this study examines numerous hurricane hazard, exposure and vulnerability quantities to determine whether the inclusion of socioeconomic data into a statistical loss-prediction model improves our ability to predict losses. Additionally, we developed a novel, loss-based hurricane classification scheme, which, if applied prior to forecast landfall, may communicate potential losses more accurately than Saffir–Simpson, thereby providing a usable preparedness tool for governments, disaster management agencies, and the financial sector. Here, 'usable' means skilfully

communicating where the expected loss would rank in the context of historical events and revising this estimation as hurricane forecasts evolve (i.e., with shorter lead times). This information could support effective preparedness by response agencies and adequate capital mobilisation by financial institutions and stakeholders. We address the following research questions:

- Which single hazard, exposure and vulnerability variable(s) exhibit the highest correlation(s) to historical U.S. hurricane losses?
- How skilful is a combination of hazard, exposure and vulnerability data in predicting historical U.S. losses compared with hazard-only predictions?
- How skilfully does a loss-based hurricane classification scale represent historical U.S. losses?

This paper is structured as follows: datasets and methods are described in section 2, results presented in sections 3–5, with a novel loss-based hurricane scale evaluated in section 6, and discussion and conclusions presented in section 7.

2 Data and methodology

2.1 Data

In this section, we describe the datasets used to provide loss, hazard, exposure and vulnerability information for historical hurricanes affecting the U.S. Fig. 1 provides a summary of these datasets and the temporal coverage spanned by each.

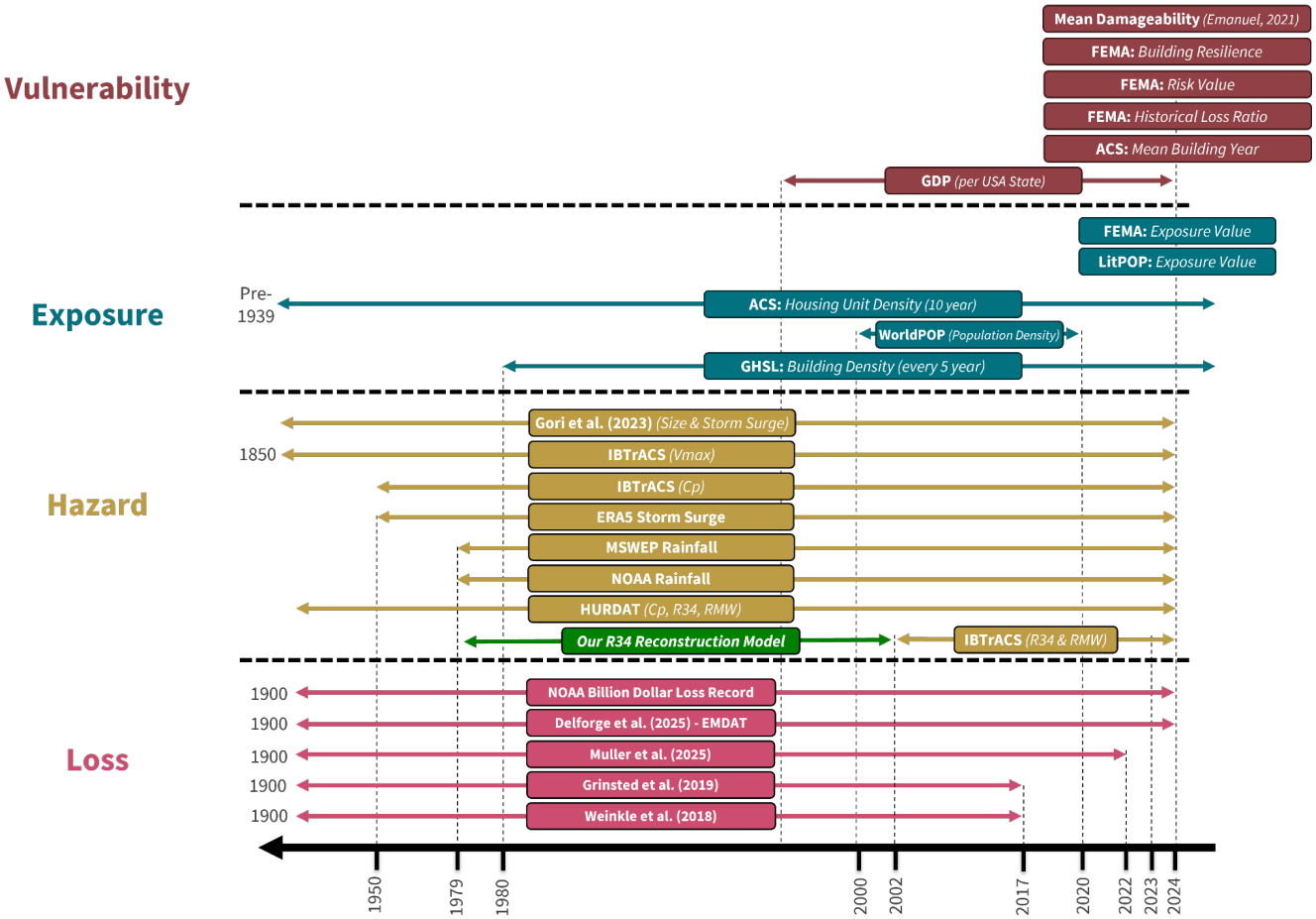

Figure 1. Schematic overview of datasets used in this study. Hazard, exposure and vulnerability predictors were combined, with loss estimates being the predictand. Time-invariant exposure and vulnerability datasets are shown with no arrows. Note that the x-axis timeline is not linear. Table S1 provides additional information and references for these datasets.

112 *2.1.1. Normalised historical hurricane losses*

113 Various sources of historical hurricane loss information exist, but no consensus reference dataset. We collated the following
114 published sources: Blake *et al*. (2011), Weinkle *et al*. (2018), Grinsted *et al*. (2019), Muller *et al*. (2025), National Centers for
115 Environmental Information (2025), and the Emergency Events Database (EM-DAT; Delforge *et al*., 2025). These datasets
116 differ in temporal coverage, reporting methodology, treatment of damage components, and inclusion of historical hurricane
117 events (Fig. 1; Table 1). To maximise sample size, we combined these datasets and, for events with multiple loss estimates,
118 these were averaged to avoid treating any dataset preferentially and help capture uncertainty. For hurricanes which made
119 multiple landfalls, losses were averaged from the two sources—Grinsted *et al.* (2019) and Muller *et al.* (2025)—that provide
120 per-landfall losses. Collating data in this way yielded 134 loss estimates for landfalling (including multiple landfalls)
121 hurricanes for the period 1979–2024, of which all variables are available for 106 events (Table 1).

122 *Table 1. Summary of hurricane loss datasets, the number of U.S. hurricane landfalls (including multiple landfalls) during*
123 *1979–2024 for which a loss estimate is available, and the subset of these landfalls for which all predictors (hazard, exposure*
124 *and vulnerability) are available.*

Dataset reference	**Dataset coverage**	**Landfalling hurricanes (1979–2024) with a loss estimate**	**Landfalling hurricanes (1979–2024) with all hazard, exposure, vulnerability and loss data**
National Centers for Environmental Information (2025) (≥ bn loss)	1850–present	58	21
EM-DAT (Delforge *et al.,* 2025)	1900–present	74	57

Muller *et al*. (2025)	1979–2022	33	33
Weinkle *et al*. (2018)	1900–2018	59	57
Grinsted *et al*. (2019)	1900–2018	102	76
All data sources	1979–2024	134	106

Economic loss estimates must be calibrated to present-day levels of damage, including adjustment factors to account for temporal changes in inflation, wealth and building density (Weinkle *et al.*, 2018). Typically, normalisation is based on country-level adjustments and assumes building density may be represented by residential housing changes. Regional variations in these factors, temporal changes in building vulnerability or commercial building density, and the impacts of climate change may not be accounted for (Muller *et al*., 2025). Each dataset we used (Table 1) provides un-normalised and normalised hurricane loss estimates. However, uncertainty arises due to the differing normalisation methodologies and reference years between datasets. To ensure consistency, we used un-normalised data and applied a unified normalisation approach, based on Weinkle *et al.* (2018) and Muller *et al.* (2025), where loss estimates were adjusted using country-level inflation and real-wealth-per-housing-unit factors (both as of 2024), and a county-level housing unit density factor (Eq. 1).

$$\boldsymbol{L_{2024}} = \boldsymbol{L_y} \cdot \boldsymbol{I}_{\frac{2024}{y}} \cdot \frac{\boldsymbol{W}}{\boldsymbol{Hn}_{1+\frac{(2024-y)}{y}}} \cdot \boldsymbol{Hn}_{1+\frac{(2024-y)}{y}} \quad \text{(Eq. 1)}$$

where L is loss per hurricane (and year), y, I is inflation, W is real national wealth per housing unit, and Hn is housing unit density. I was determined using the annual implicit price deflator for gross domestic product provided by the U.S. Federal Reserve Bank of St. Louis for the period 1979–2024 (U.S. Bureau of Economic Analysis, 2023). Hn density was determined

within R34 using U.S. housing unit data (U.S. Census Bureau, 2024). *W* was quantified using an estimate of current-cost net stock of fixed assets and consumer durable goods (U.S. Bureau of Economic Analysis, 2025).

2.1.2. Hazards

Hurricane track location, intensity and size information was obtained from the International Best Track Archive for Climate Stewardship (IBTrACS) v04r01 (Gahtan *et al.*, 2024), provided by the National Hurricane Center (NHC), part of the NOAA. For each historical hurricane, we obtained 1-minute sustained maximum wind speed, v_{max}, minimum central sea-level pressure, c_p, translation speed, radius of maximum wind (from the storm centre), RMW, and the outermost radii of 34-, 50- and 64-knot wind speeds from the storm centre), respectively, R34, R50 and R64. Each quantity was determined at the timestep before the storm centre crosses over land, so atmospheric fields are minimally impacted by land-surface interactions. However, IBTrACS data are incomplete (i.e., not all hazard variables are available at every timestep for every hurricane). Therefore, we supplemented IBTrACS with data from NOAA's HURDAT2 reanalysis (Landsea and Franklin, 2013)—specifically, the 'U.S. Hurricane Impacts / Landfalls' table of landfall information collected by NOAA reconnaissance aircraft (Hurricane Research Division, 2025), and from Gori *et al*. (2023). Where data are missing in IBTrACS, HURDAT2 data were substituted, if available. Where data are available in IBTrACS and HURDAT2 at a given timestep, HURDAT2 data were prioritised.

Storm surge and rainfall cause damage through coastal and inland flooding. In this study, historical hurricane storm tide (maximum storm surge and tidal height) data were taken from the storm surge residual product (Copernicus Climate Change Service, 2022), derived using the Global Tide and Surge Model (version 3.0; Kernkamp *et al*., 2011; Wang *et al*. 2021) forced by European Centre for Medium-Range Weather Forecasts' fifth-generation reanalysis (ERA5; Hersbach *et al.*, 2020). This provides hourly reconstructed historical storm tide height from 1950–present. Storm tide residual is calculated as the difference between the total water level and simulated storm-tide elevation, including the influence of storm surge and tide. Storm tide may be larger in the hours before or after a hurricane makes landfall, depending on antecedent tidal height. To account for this, we defined the maximum storm tide residual as the maximum along the U.S. coastline within a 1,000 km radius of the hurricane's central coordinate and 24 hours before and after a hurricane makes landfall. An example maximum storm tide residual for Hurricane Katrina (2005) is shown in Fig. S1.

Historical hurricane-related rainfall footprints were derived from the Multi-Source Weighted-Ensemble Precipitation (MSWEP) dataset (Beck *et al.*, 2019), which assimilates gauge observations and satellite data to reconstruct 3-hourly rainfall 1979–present. For each hurricane, we determined total accumulated rainfall, maximum 3-hourly rain rate, and maximum total rain accumulation per grid-point along the track, each within a 500-km radius of the hurricane centre (location taken from

IBTrACS) at each timestep. An example rainfall accumulation footprint for Hurricane Katrina is shown in Fig. S2. This chosen radius is based on previous research (e.g., Stansfield and Reed, 2023), although a fixed radius may lead to some overestimation of cyclone-related precipitation (Stansfield *et al*., 2020). To complement MSWEP, the maximum rainfall accumulation along each hurricane track was collated from National Oceanographic and Atmospheric Administration (2025), providing single maximum rainfall accumulation values, although not allowing differentiation between multiple landfalls with this dataset.

This study considers only landfalling hurricanes, excluding bypassing hurricanes. It is difficult to obtain a comparable measure of hurricane intensity for a bypassing event because its intensity, measured close to the system center, is over ocean and may therefore be relatively high compared with a directly landfalling event. It is necessary to avoid introducing such an artifact into our statistical model.

2.1.3. Exposure

We took county-level building value information across the U.S. from the National Risk Index (Federal Emergency Management Agency, 2024), derived from Hazus 6.1 (Federal Emergency Management Agency, 2024a), providing 2022-relative valuations per county based on the 2020 U.S. Census. Building values are time-invariant. Near present-day (2019) building value was quantified using the LitPOP dataset (Eberenz *et al.*, 2020), providing global aggregated building value estimates at a 1-km spatial resolution. Building value estimates vary between the two datasets; hence, we used two building value datasets.

We also used decadal, county-level housing unit density data (U.S. Census Bureau, 2024), available 1950–present, as well as semi-decadal building density estimates from the Global Human Settlement Layer (GHSL), providing built-up surface area data derived from Sentinel-2 composite and Landsat satellite imagery from 1975–present at 1-km spatial resolution (Pesaresi and Politis, 2023). Annual gridded population density data between 2000 and 2020 at 1-km spatial resolution were obtained from WorldPop (WorldPop, 2018). For hurricane landfalls outside the temporal coverage of GHSL and WorldPop, we used data for the closest available year. Therefore, a limitation to highlight is that we overestimate population density for pre-2000 events.

2.1.4. Vulnerability

Structural vulnerability—the susceptibility of buildings to damage—is influenced by building age, often used as a proxy for building condition and resilience, and related to changes in building codes (regulated construction standards that include a

minimal resistance to extreme weather). We used county-level average building age data (U.S. Census Bureau, 2024) and a county-level indicator of building resistance to extreme weather (Federal Emergency Management Agency, 2025). We also used county-level Hurricane Risk Score and Hurricane Historical Loss Ratio data from Federal Emergency Management Agency (2024b) and Zuzak *et al.*, (2021). Hurricane Risk Score is defined as the average social vulnerability (i.e., extent to which specific social groups are disproportionately susceptible to hurricane impacts) and community resilience (i.e., capacity to prepare for, withstand, and recover from hurricane hazards), and is given as a percentage. Hurricane Historical Loss Ratio is defined as the percentage of a location's exposed value damaged by past hurricanes. We quantified the mean Hurricane Risk Score and Hurricane Historical Loss Ratio across all counties within several hurricane radii (R34, R50 and R64—see section 2.2.). GDP data for each affected U.S. state per year, indicating a state's resilience resources, for the period 1998–2024 (U.S. Bureau of Economic Analysis, 2025) were used, and 1998 GDP values were applied to pre-1998 events.

Hurricane wind vulnerability may also be expressed as a logistic–cubic wind–damage function, relating wind speed to the fractional value of assets lost. This study uses a simple quantification of this (Eq. 2 and Eq. 3), which was deduced by Emanuel (2011).

$$\boldsymbol{f} = \frac{\boldsymbol{v_n^3}}{\boldsymbol{1+v_n^3}}, \quad \text{(Eq. 2)}$$

where f is the fraction of the property value lost and v_n is defined as:

$$\boldsymbol{v_n} = \frac{[(\boldsymbol{v-v_{thresh}}),\boldsymbol{0}]}{\boldsymbol{v_{half}-v_{thresh}}}, \quad \text{(Eq. 3)}$$

where v is maximum wind speed, and v_{thresh} and v_{half} are the thresholds at which no asset damage and half asset damage occur, respectively. Building characteristics (e.g., construction type and age) influence vulnerability curves, and Vickery *et al*. (2006) and Federal Emergency Management Agency (2024a) suggest v_{half} values in the range 120–160 kts. In this study, damage estimates were computed for historical hurricanes using this single vulnerability function for all buildings, with v_{thresh} = 40 kts and v_{half} = 140 kts. However, weaker systems may be damaging, such as tropical depression Allison (2001), modelling suggests v_{half} may be as low as ~50 kts (Federal Emergency Management Agency, 2024a). Multiple vulnerability functions for different building types cannot be applied due to incomplete localised building characteristic data. Instead, asset damage potential was applied to 1-dimensional LitPOP exposure and GHSL building density data within each hurricane footprint to estimate the

exposure value and number of buildings damaged. At each timestep, v_{max} was used with Eq. 2 and Eq. 3 (Emanuel, 2011) and the extracted exposure and building density, allowing v_{max} to vary with time.

2.2. Methods

2.2.1. Statistical estimation of hurricane size

Hurricane size (i.e., R34, R50 and R64) data are only available in IBTrACS from 2002 onwards. This is a significant constraint for studies of impact, as size information is needed to determine the region impacted by an event—i.e., its footprint. The exposure and vulnerability impact footprints derived in this study require hurricane size estimates. To estimate size prior to 2002 and extend the sample of landfalling hurricanes for this study, we developed a skilful random-forest statistical model to estimate R34, R50 and R64 for each hurricane and at each timestep, based on v_{max}, RMW, c_p and latitude (Fig. 2), with RMW found to be the most influential predictor. When R34 estimates from this model are compared with R34 observations from 2002 onwards, a Spearman's correlation coefficient, ρ, of 0.85 and a mean absolute error (MAE) of 24.5 nm were found (Fig. 2). This evaluation used a leave-one-out approach (i.e., the prediction model was trained on all observations except one, and skill evaluated on the left-out observation) across 3,984 timesteps (for which R34, v_{max}, RMW, c_p and latitude within IBTrACS are not missing). There is a slight underestimation of R34 at lower values and slight overestimation at higher values, but the model overall performs well. This statistical modelling is a skilful supplement to missing IBTrACS data (Fig. 2 and Fig. S3) and allows storm size estimation back to 1979, which more than doubles our historical hurricane event sample size. Prediction models were also developed to estimate R50 and R64 for historical storms, where observations are available, with evaluation shown in Fig. S3.

From 1979 to 2002, however, there are instances where RMW data are missing from IBTrACS (v_{max}, RMW, c_p and latitude are less often missing). So, for these timesteps, we either substituted the missing RMW value from the corresponding value from HURDAT2, or obtained the RMW value from reconstructions of Gori *et al.* (2023). Reconstructed RMW (Gori *et al.*, 2023) is based on the hurricane wind model of Chavas *et al.* (2015) and ERA5 data. Of all 3-hourly timesteps where a hurricane is over land between 1979 and 2002 (approximately 10,000 timesteps), approximately 25% timesteps have a missing RMW estimate from each of these three datasets. In these instances, we replaced the missing value with the RMW from the previous timestep. Although this introduces uncertainty, R34, R50 and R64 estimates from the random-forest model using RMW

241 estimates from previous timesteps are also a function of c_p, v_{max} and latitude, quantities that are much less frequently missing
242 in IBTrACS, and these constrain our R34 statistical model even when using substituted RMW values.

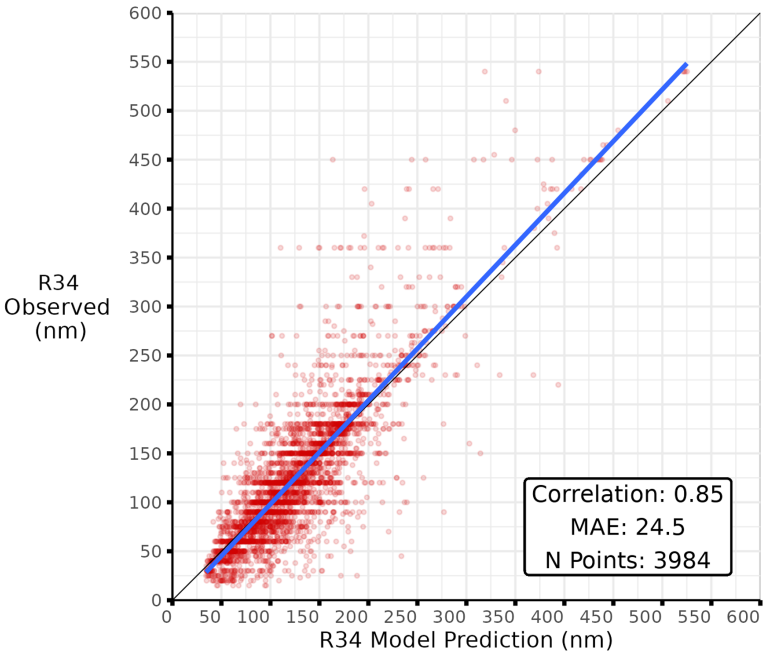

243

244 *Figure 2. Comparison of estimated and observed hurricane R34 (unit is nautical miles, nm) for the period 2002–2023. Our*
245 *random-forest statistical model uses hurricane v_{max}, RMW, c_p and latitude as R34 predictors.*

246 *2.2.2. Extracting hurricane-centred exposure and vulnerability footprints*

247 For each hurricane, exposure and vulnerability data were extracted within the R34, R50 and R64 radii at each timestep, and
248 accumulated to create two impact footprints: i) along the full hurricane track where v_{max} > 34 kts (Fig. 3) and ii) from the

immediate landfall location (i.e., up to 12 hours after landfall). Hurricanes weaken over land, so obtaining two impact footprints captures the immediate landfall, where intensity influences impacts most strongly, and the full hurricane track.

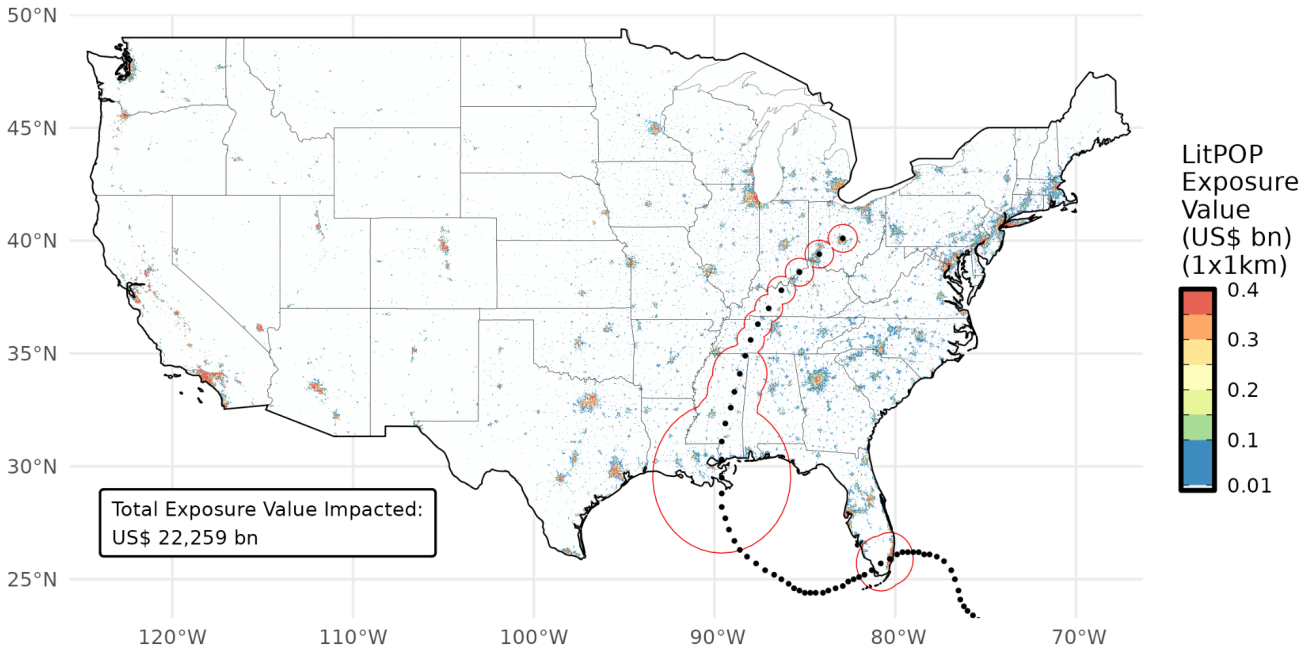

Figure 3. Example LitPOP exposure value impact footprint of Hurricane Katrina (2005). Hurricane locations from IBTrACS every three hours are shown as black dots, with the R34 radius around the hurricane centre indicated by the red lines. Harvey made landfall in southern Florida, traversed the Gulf of Mexico, and made a second landfall in Louisiana.

2.2.3. Predictive statistical approaches

We assessed the skill of three independent statistical approaches to predict hurricane loss, each based on the same set of inputs. These are: (i) a weighted combined-rank framework, (ii) a linear-regression framework, and (iii) a random-forest decision-tree framework. Our target predictand is average loss per hurricane, derived from multiple datasets (see section 2.1.1.). Overall, 106 hurricanes, for which all risk variables could be quantified (Table 1), were used to train our predictive model. To evaluate the skill of the linear regression and random-forest predictive models, leave-one-out cross-validation was used, where each input case was treated once as the test case and the model trained on the remaining cases. The leave-one-out approach is better suited to evaluating the skill of single predictions than, for example, k-fold cross-validation, where input data are split into

training subsets. For the weighted combined-rank framework, which determines the combined loss rank from various hazard, exposure and vulnerability ranks, such validation is inappropriate, as the combined-rank approach does not require training data. Instead, optimal combinations of weights between -10 and 10 were determined for each combination of input variables, to minimise a cost function, which in this case was the model root-mean-square error (RMSE) between predicted and observed hurricane loss rank.

Two approaches were considered for representing input variables: raw values and ranked values. As input variables span disparate ranges (e.g., c_p spans 900–1000 hPa; LitPOP exposure spans U.S.$ 10 M to 1 tn), raw values were normalised to the same scale as ranked values 1–*n* (i.e., 1–106). In this normalisation, each variable was linearly rescaled to assign the maximum value a score of 1 and minimum a score of 106, with intermediate values mapped proportionally between these bounds. Linear and normalised input predictor ranks were derived, with rank 1 corresponding to the costliest event and rank 106 to the least costly. To predict each hurricane's loss, the equivalent predicted loss rank and observed loss rank were identified, with the loss from that observed hurricane being attributed to that predicted loss rank.

We quantified model performance with the Spearman correlation coefficient, ρ, testing the ordering of prediction according to correlation between ranked values (i.e., whether one event is more damaging than another), Pearson correlation coefficients, *r*, testing non-ranked correlation, and RMSE. Spearman's ρ and RMSE were used as ρ is a good indicator of the capability of accurately predicting loss rank, but not suitable for identifying cases where large differences occur in the loss prediction of a single hurricane.

3 Historical relationship between hurricane wind speed and loss

Hurricane-related losses across the U.S. have generally increased over time and exhibit large interannual variability (Fig. 4). The most destructive year for losses was 2005, with U.S.$ 153 bn in un-normalised (and approximately U.S.$ 350 bn in normalised) loss. The most damaging event was Hurricane Katrina (Fig. 5), although uncertainty is evident across available loss datasets (Table 1). If Katrina occurred today, loss may be in the range of U.S.$ 190–290 bn (Fig. 5). Katrina, however, is one of numerous high-impact hurricanes whose v_{max}-based Saffir–Simpson category at landfall is at odds with the magnitude of associated loss (Bloemendaal *et al*., 2021). Katrina was a category-3 landfall, despite causing unprecedented, record-breaking damage (Fig. 5). Other cases whose damage is mismatched with their Saffir–Simpson category include category-1 Hurricane Sandy (2012) and category-2 Hurricane Ike (2008), which each caused substantial losses (Fig. 5). Additionally, Hurricane Harvey (2017) was a category-4 landfall and the second-most damaging hurricane, but its loss is uncertain, with

estimates between U.S.$ 90–190 bn. The historical record reveals the limitation of an event's Saffir–Simpson category in conveying its loss.

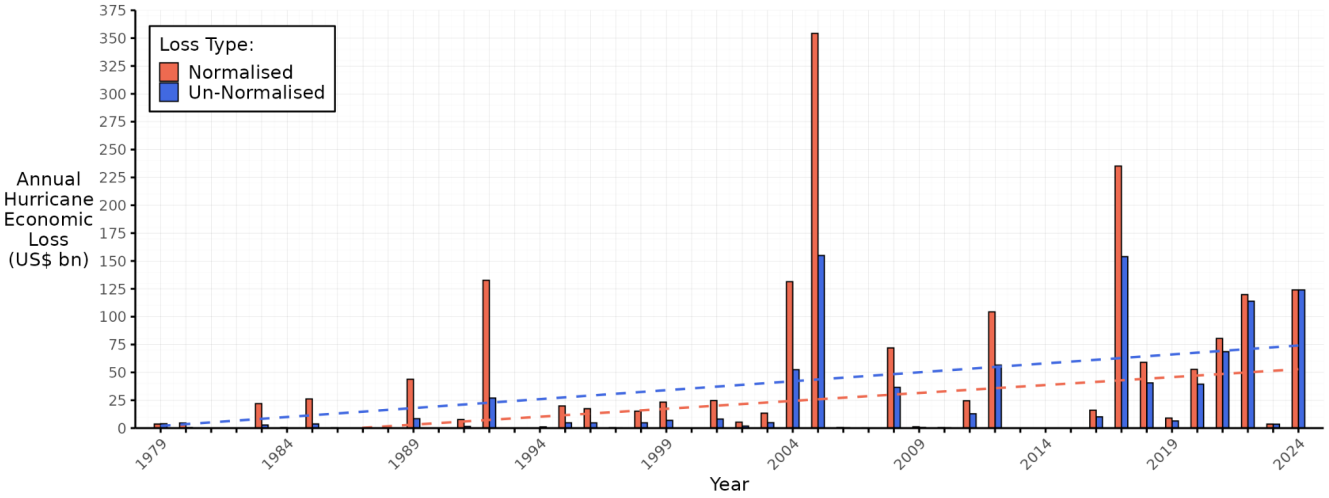

Figure 4. Average historical U.S. hurricane-related losses, (red) normalised to 2024 and (blue) un-normalised by inflation, wealth and housing unit density (blue). Dashed lines indicate upward linear trends.

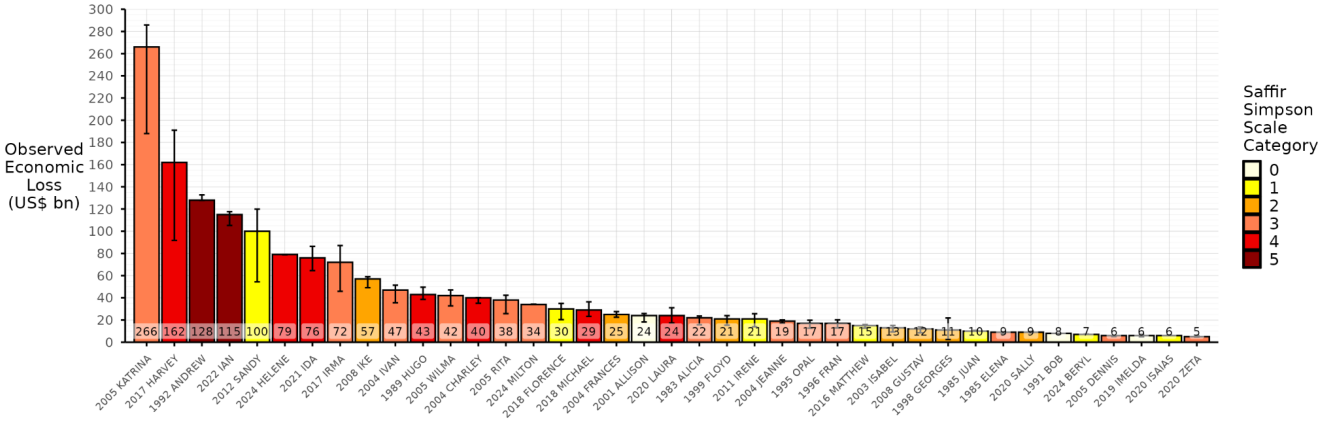

297

298 *Figure 5. Average loss per hurricane, normalised to 2024, for loss events exceeding U.S.$ 5 bn. Error bars indicate the range*
299 *in loss estimates across datasets (Fig. 1 and Table 1) and colour indicates landfall Saffir–Simpson category.*

300 Although loss generally increases with the Saffir–Simpson landfall category and therefore wind speed (Fig. 5), the Saffir–
301 Simpson scale has limited skill in predicting loss (Fig. 6a), with a correlation of $\rho = 0.53$ across 106 events (RMSE = U.S.$
302 17.1 bn when using Saffir–Simpson category to predict loss rank and associated loss using a linear model). Using v_{max} to
303 predict normalised hurricane loss yields a correlation of $\rho = 0.52$ (RMSE = U.S.$ 17.6 bn), which is slightly lower (Fig. 6b)
304 and consistent with Klotzbach *et al.* (2020). Notably, landfall v_{max} is significantly less skilful at predicting loss for more extreme
305 storms, with generally higher error at more extreme v_{max} values (Fig. 6b), which is particularly problematic as an inaccurate
306 forecast for these more intense storms would produce larger errors in loss. The relationship between v_{max} and loss is potentially
307 nonlinear but spread, and therefore error, in loss generally increases with v_{max}. Performing a rank correlation between observed

loss and loss predicted from v_{max} reveals significant spread (and heteroscedasticity) across the observed range (Fig. 7a), and this is found for all events as well as those where exceeds U.S.$ 1 bn (Fig. S4).

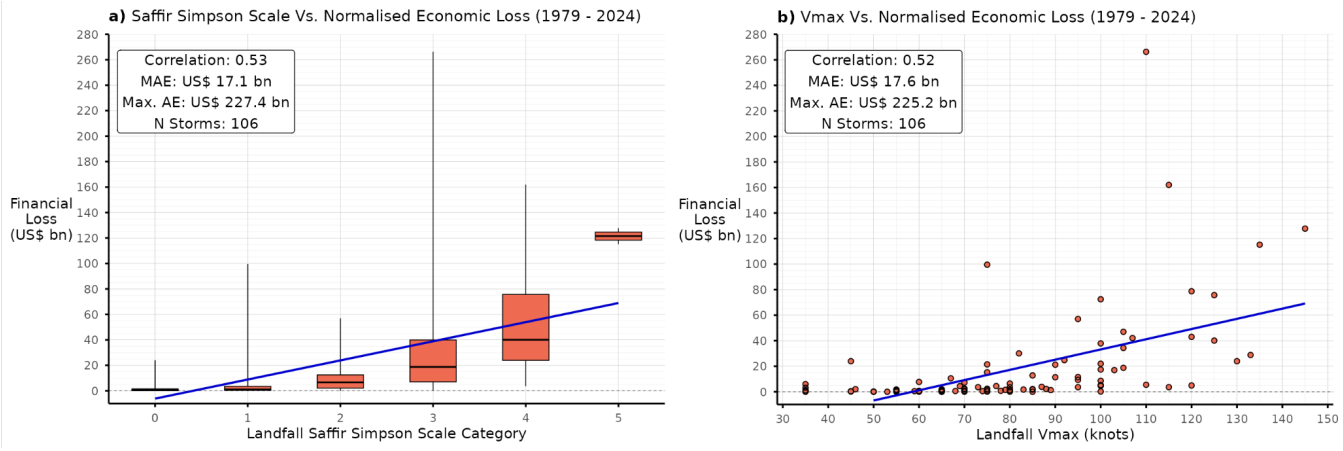

Figure 6. Average economic hurricane financial loss (normalised to 2024) versus a) Saffir–Simpson category and b) landfall v_{max} of U.S. landfalls over the period 1979–2023. Blue lines indicate linear fits and an indication of goodness of fit is given in each legend: mean absolute error (MAE), absolute error (AE), and sample size, N.

4 Historical relationships between multiple hazard, exposure and vulnerability variables and loss

We next analysed linear correlations between single predictors and historical hurricane loss over the period 1979–2024, using both raw (Fig. 7a) and rank (Fig. 7b) values. This analysis demonstrates that high prediction skill may be obtained across numerous hazard, exposure and vulnerability hurricane quantities, with landfall c_p rank yielding the highest correlation (r = -0.78), followed by GHSL building density damage percentage (r = 0.77) and LitPOP exposure value damage percentage (r = 0.74) (Fig. 7a). Overall, using the value rank per storm yields higher correlations than using raw values (Fig. 7c), particularly for exposure predictors, because using ranks normalises to a linear scale, suggesting that landfall attribute ranks may provide more skilful loss predictions. This complements the analysis of Klotzbach *et al.* (2022a), who showed that landfall c_p better correlates with loss rank than v_{max} or accumulated cyclone energy (ACE). Here, we further show that landfall c_p outperforms

other hazard variables and that landfall exposure and vulnerability variables yield higher correlations with loss rank than landfall v_{max}.

In this study, several hazard variables at landfall (v_{max}, c_p, storm tide, R34, translation speed, and RMW) remain unchanged, but variables quantified within a hurricane footprint depend on chosen hurricane size metric (i.e., R34, R50 or R64), and those quantified along-track depend on timeframe (i.e., full track or 12 hours post landfall). For landfall variables with significant correlations to loss (i.e., ≥0.3), a 12-hour post-landfall track yields similar (or somewhat higher) correlation compared with using the full track where winds exceed 34 kts (Fig. S5a). This indicates that including the full track, where winds weaken over land, reduces correlation. (Studies of inland impacts using full-track analysis may need to cope with lower skill than landfall-focussed studies.) A notable exception is the percentage of damaged GHSL building density, which has a strong correlation using the full track ($\rho = 0.78$ using R34 and $\rho = 0.79$ using R50). Correlations are generally higher when considering normalised rather than un-normalised loss (Fig. S5b). Additionally, rank correlations are similar when using R34 and R50 to

define impact radius, but correlations using R64 are lower (Fig. S5c). R64 is typically less than 100 nm, which may be too small to capture hurricane impacts, especially for lower-resolution data (e.g., county-level housing unit data).

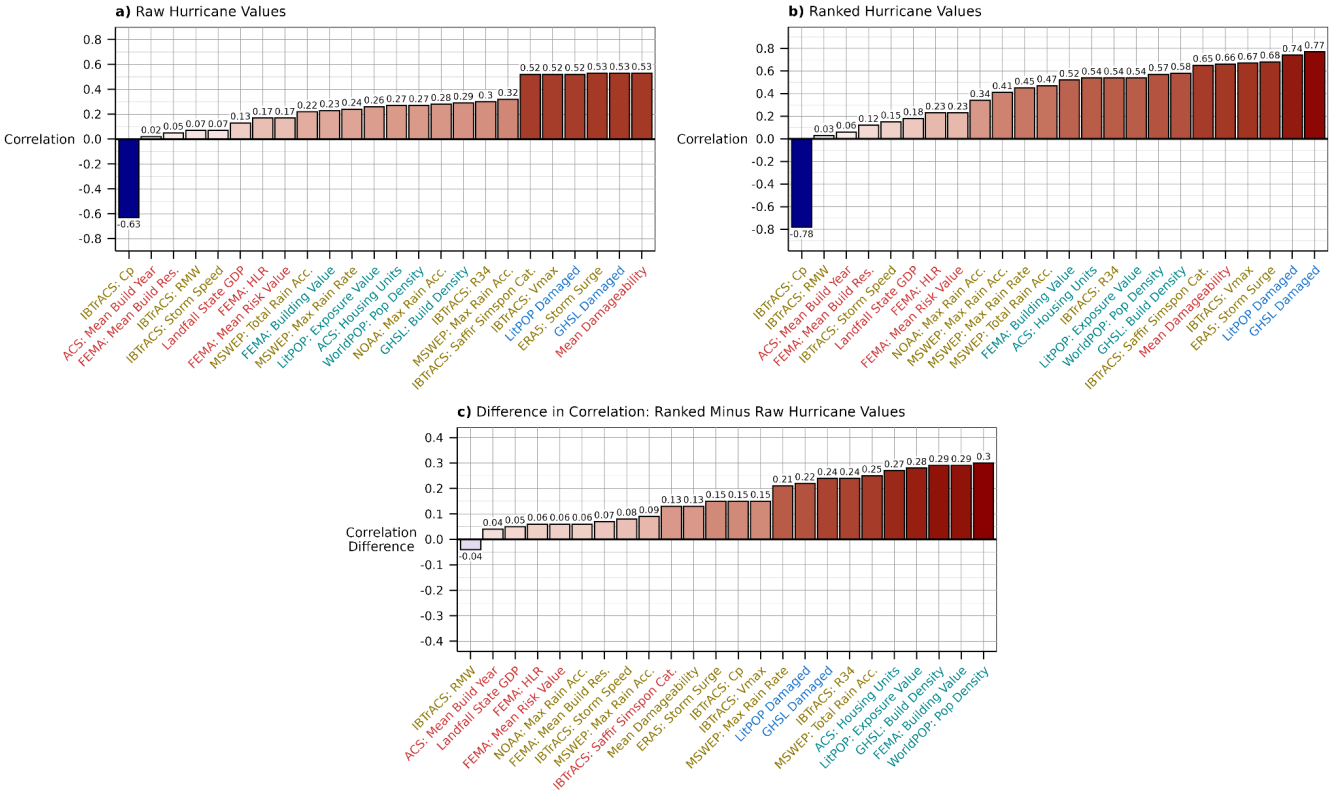

Figure 7. Pearson's correlation coefficients between historical hurricane landfall predictors, quantified at landfall and within 12 hours of landfall, and averaged loss for the period 1979–2024. Shown are (a) raw values versus loss, (b) predictor rank values versus loss, and (c) the coefficient difference between using raw versus ranked values (i.e., ranked minus raw correlations). Note that the x-axes differ between the panels due to correlation ordering. Colours indicate whether the variable is a hazard (yellow), exposure (blue) or vulnerability (red) variable (refer to Fig. 1). Note that c_p is inversely related to hurricane intensity and therefore negatively correlated with damage.

5 Statistical prediction of historical hurricane loss

Using landfall v_{max} rank to predict storm loss, by assigning the loss from the equivalent loss rank, yields $\rho = 0.54$ and RMSE = U.S.$ 35.6 bn (Fig. 8), so v_{max} has limited skill predicting historical loss. Hurricanes Katrina (2005) and Harvey (2017),

which were category-3 and category-4 landfalls, respectively (Fig. 4), are among the most underestimated losses despite being the two most damaging events since 1979 (Fig. 9a). Furthermore, using v_{max} alone leads to loss predictions exceeding U.S.$ 30 bn for several less-damaging (≤ U.S.$ 10 bn) events (Fig. 9a), including Michael (2018), Laura (2020), Dennis (2005), Andrew (1992; second landfall) and Idalia (2023). Our analysis (Fig. 7) and recent work (Klotzbach *et al.*, 2020; Klotzbach *et al.*, 2022a), show landfall c_p to be the most skilful single hazard predictor for historical loss, and using landfall c_p rank to predict loss rank improves this correlation ($\rho = 0.78$ and RMSE = U.S.$ 26.4 bn) (Fig. 8). However, several events, across a range of observed losses, remain poorly predicted: Andrew (1992), Michael (2018), Rita (2005), Hugo (1989), Dennis (2005), Allen (1980) and Idalia (2023) are all overestimated (Fig. 9b). This greater predictive skill of c_p over v_{max} is likely due to the physical pressure–wind balance intrinsic to hurricanes (Chavas *et al.*, 2017), but intensity metrics alone cannot accurately model loss.

We now combine landfall hazard, exposure and vulnerability quantities to derive more skilful models to predict historical hurricane loss, using three statistical approaches: multiple linear repression, random-forest, and weighted combined rank (Fig. 8). Using a random-forest model based on the optimal combination of hazard, exposure and vulnerability predictors is significantly skilful ($\rho = 0.85$; RMSE = U.S.$ 18.7 bn), with a slight improvement obtained from using a linear-regression model ($\rho = 0.87$: RMSE = U.S.$ 17.1 bn) (Fig. 8). Further skill is obtained when using a weighted combined-sum approach ($\rho = 0.89$; RMSE = U.S.$ 7.0 bn), representing a large decrease in RMSE when compared to using c_p and v_{max} (Fig. 8). Overall,

effectively combining hazard, exposure and vulnerability predictors is found to significantly reduce RMSE by as much as ~67% compared with using landfall v_{max} rank alone, and by ~55% when using landfall c_p rank alone (Fig. 8).

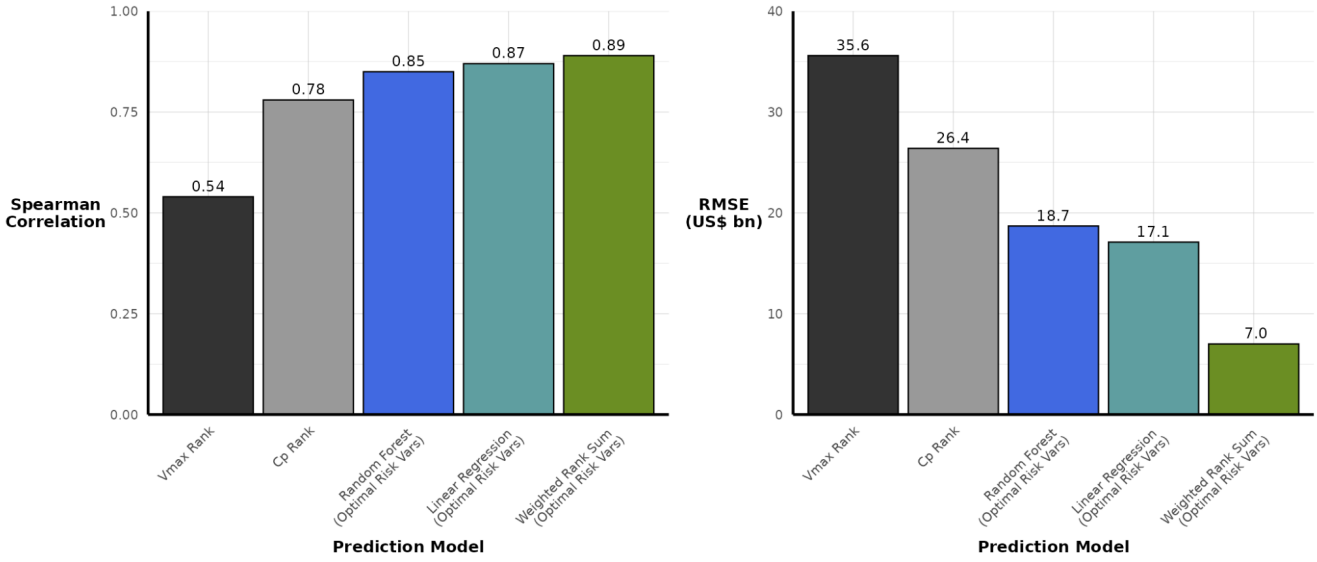

Figure 8. The a) Spearman's correlation coefficient, ρ, and b) root mean squared error (RMSE) of each tested historical hurricane loss-prediction model.

This optimal model uses the combined normalised ranks of landfall c_p, maximum rainfall accumulation, and the percentage of total GHSL building density loss within R64 of the hurricane centre and within 12 hours of landfall (Fig 8; Fig. 9c). This model includes two hazard quantities representing hurricane wind and inland flooding intensity (c_p and rainfall), with hurricane radius implicitly included in the percentage of total GHSL building density damage (with storms with larger R64 having higher impacted building density values). This also includes exposure values of impacted building density and applies a vulnerability function, by determining the percentage of damaged buildings proportional to v_{max} (at each timestep). The inclusion of building density within R64 indicates some prediction skill from capturing the inner region of a hurricane, where wind-induced damage to buildings may be highest, but only in combination with other factors. Overall, this model demonstrates the extent to which loss prediction skill can be improved when accounting for hazard, exposure and vulnerability.

Across our sample of 106 historical hurricanes, this prediction model has the lowest RMSE (U.S.$ 7.0 bn) when hazard, exposure and vulnerability predictors are ranked and summed, while also applying optimal weights (Fig. 8c). Moreover, for

highly damaging historical hurricanes (≥ U.S.$ 20 bn), $\rho = 0.9$, which is significantly higher than using only landfall v_{max} ($\rho = 0.45$) or c_p ($\rho = 0.66$) (Fig. 9). Our optimal model results in the five most-damaging hurricanes (Katrina, Harvey, Andrew, Ian, and Sandy) being ordered according to observed losses and thus well captured, and higher-loss events (≥ U.S.$ 20–80 bn) overall are skilfully predicted. However, some discrepancies remain. The largest errors include hurricanes Michael (2018), Opal (1995) and Allen (1980), all of which have a high landfall c_p rank (i.e., high intensity) but relatively low loss. Overall,

this model is markedly more skilful than using intensity metrics (landfall v_{max} and c_p) to predict historical losses (Fig. 8 and Fig. 9).

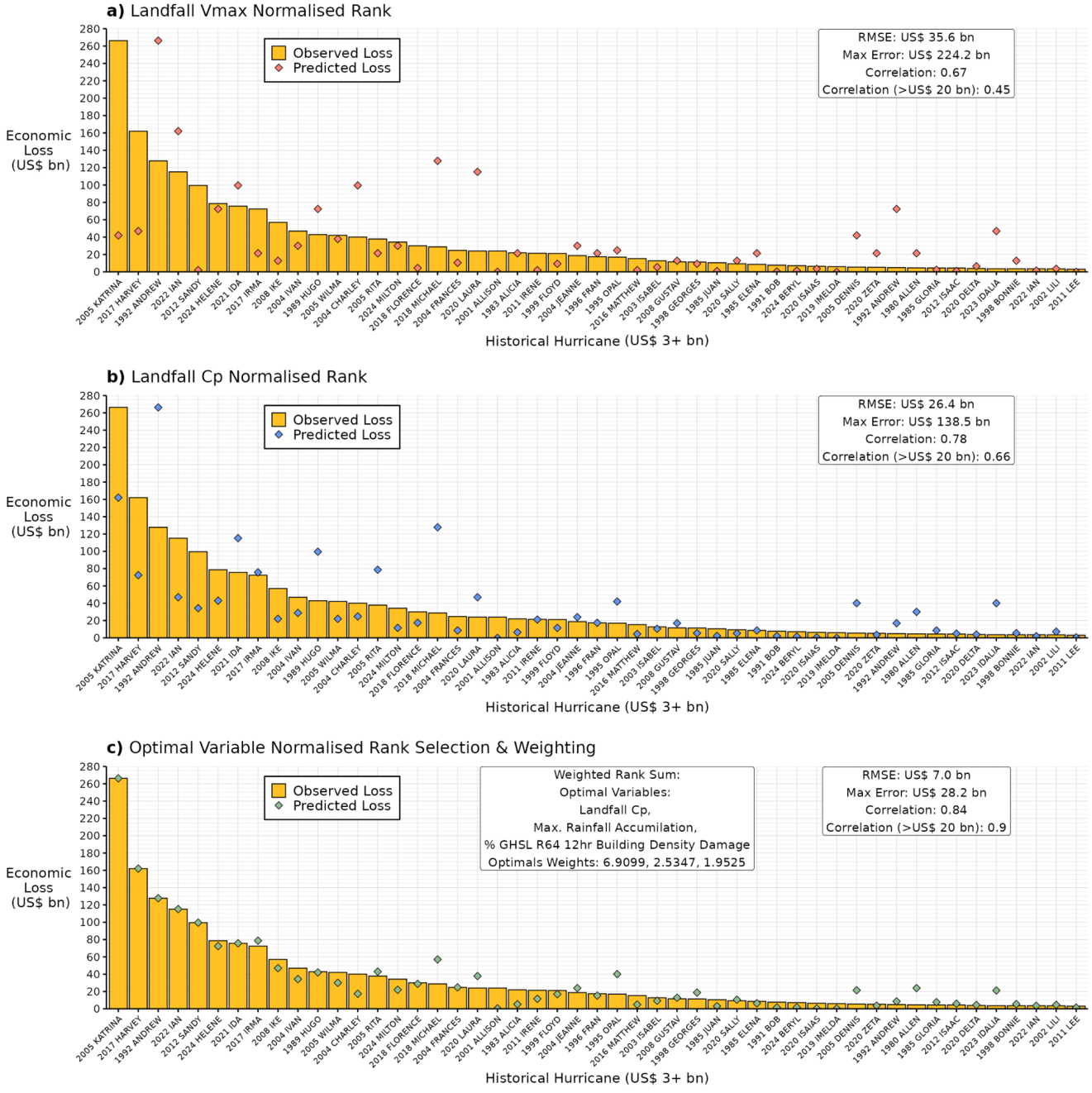

Figure 9. Comparisons of landfall predictor rank with loss rank to predict past hurricane loss given past loss observations, using (a) landfall v_{max} rank, (b) landfall c_p rank, and (c) optimally selected and weighted (refer to Fig. 7) hazard, exposure and vulnerability linear rank variables at landfall. Yellow bars indicate observed historical hurricane loss and the coloured diamonds indicate predicted historical hurricane loss. Note that the optimal risk predictors and their optimal weights are given in panel (c).

6 A loss-based hurricane classification

The Saffir–Simpson scale is an effective communication tool and a key component of early-warning dissemination (Camelo and Mayo, 2021; Oliver-Smith, 2020; Wehner and Kossin, 2024), but, being based on v_{max} alone, does not correspond adequately with historical loss ranking (Fig. 4, Fig. 5). Based on our analyses, we devised a loss-based hurricane categorisation, termed the 'Hurricane Predictive Loss Scale' (HPLS). We intend this scale to complement the Saffir–Simpson scale, as well as published work (e.g., Bloemendaal *et al.*, 2021; Pilkington and Mahmoud, 2016), and be a classification scheme that may be used by stakeholders, particularly (re-)insurance, to predict loss.

Since 1900, 39% of landfalling hurricanes have been category 1, with 12% and 3% being category 4 and 5, respectively (Table S2). We applied the observed relative proportions in each Saffir–Simpson category to averaged historical loss data since 1979 (Table 1) to derive historical loss categories (Table 2) for the HPLS. As examples, a hurricane with loss less than U.S.$ 1.3 bn is a 'loss category 1' event and an event causing loss greater than U.S.$ 119.5 bn is a 'loss category 5' event.

Table 2. Percentage of landfalling historical storms within each Saffir–Simpson category since 1900 (Hurricane Research Division, 2025). Loss category thresholds used to define the proposed HPLS.

Saffir–Simpson category	**Frequency**	**% of all hurricanes**	**v_{max} threshold (kts)**	**HPLS loss category threshold (U.S.$ bn)**
1	84	38.9	64-83	0-1.3

2	54	25.0	83-96	1.3-5.3
3	46	21.3	96-113	5.3-29.5
4	26	12.0	113-136	29.5-119.5
5	6	2.8	136+	119.5+

Using our skilful hurricane loss-prediction model, we determined the HPLS loss category derived from the predicted losses for each historical hurricane (Fig. 9c and Fig. 10). The ranks of the most damaging hurricanes (Katrina, Harvey, and Andrew) are correctly predicted as being 'loss category 5', and the next most damaging storms (Ian to Wilma) are 'loss category 4' events, with losses between U.S.$ 115-42 bn (Fig. 10). Hurricane Sandy (2012), which is under-categorised by the Saffir–Simpson scale (category 1) and the 'Tropical Cyclone Severity Scale' (Bloemendaal *et al.*, 2021) (category 2), is a 'loss category 4' event in our scheme. Combining hazard, exposure and vulnerability quantities and loss-based categorisation is more skilful for many cases than is possible based only on hazard information.

The most damaging hurricane that is misrepresented by the HPLS scheme is Hurricane Charley (2004), whose observed loss (U.S.$ 40.1 bn) is underpredicted by our model (Fig. 10). Charley should be 'loss category 4' (Fig. 4 and Table 2), but its predicted loss (~U.S.$ 20 bn) falls in 'loss category 3'. Additionally, tropical storm Allison (2001) is assigned to 'loss category 1', which stands out as a poor model prediction (Fig. 10). Overall, we found 74 events (70%) are correctly classified by the HPLS (Table 3). However, 28 events (26%) are misrepresented by ±1 'loss category' and 4 (4%) are misrepresented by ±2

416 ‘loss categories’ (Table 3). By comparison, Saffir–Simpson categories represent just over half (55%) of events correctly, and
417 31%, 12% and 2% are misrepresented by ±1, ±2 and ±3 ‘loss categories’, respectively (Table 3).

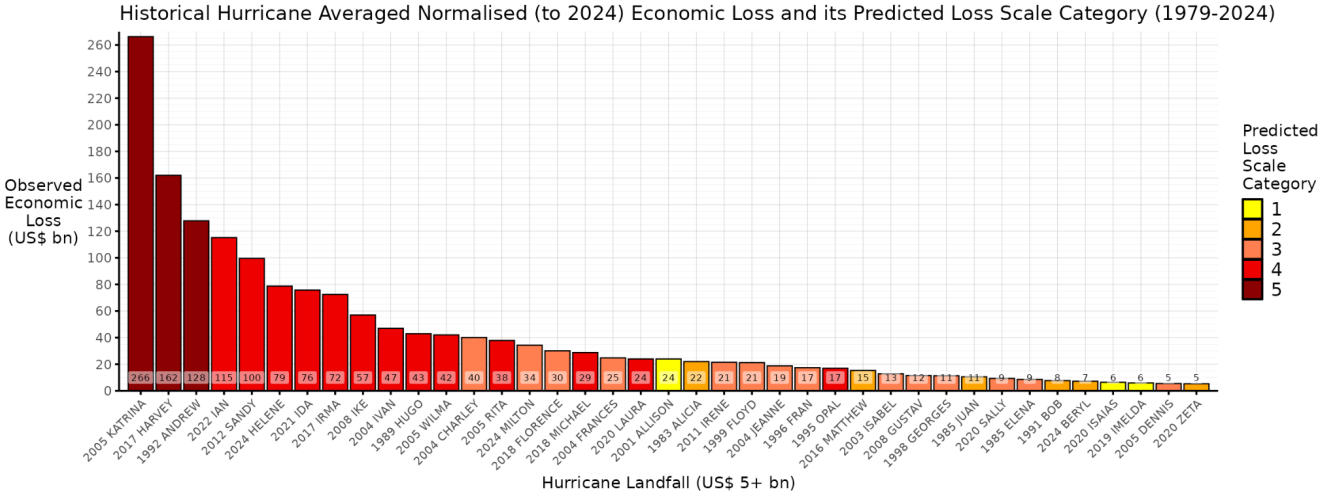

418

419 *Figure 10. Predicted ‘loss category’ of each historical landfalling hurricane, using the optimal prediction model (Fig. 9c) and*
420 *the HPLS (Table 2).*

421

Table 3. Quantified differences between Saffir–Simpson category or predicted 'loss category' using our model (Fig. 9c) and the observed 'loss category' from the HPLS (i.e., derived from observed loss).

Difference from observed 'loss category'	**Saffir–Simpson category**	**Predicted 'loss category'**
0 (i.e., correct prediction)	58 (55%)	74 (70%)
±1	33 (31%)	28 (26%)
±2	15 (12%)	4 (4%)
±3	5 (2%)	0 (0%)

7 Summary and discussion

This study explored statistical relationships between historical U.S. hurricane-related losses and quantities describing hazard, exposure and vulnerability, and makes two contributions. First, we determined whether the inclusion of socioeconomic information into a predictive model for loss from U.S. landfalls yields significant additional skill compared with using only hazard information. For historical hurricanes, we derived storm-centred hazard, exposure and vulnerability quantities, and limited our analysis to cases for which observed loss estimates are available and hurricane radius is either observed or could be skilfully estimated statistically from other observed size information. Second, we devised a loss-based hurricane classification scheme to allow rapid, skilful assessment of the loss potential of forecast events, which is intended for use by

stakeholders in hurricane risk, including governmental agencies and the (re-)insurance sector, and complements existing classification schemes.

7.1 Key results and limitations

7.1.1 Integrated hazard, exposure, and vulnerability data predict historical hurricane losses more skilfully than hazard data alone

Although historical losses generally increase with landfall wind speed (and Saffir–Simpson category), hazard information alone has insufficient skill in predicting historical losses, with a large RMSE across all events, a finding which substantiates previous research (Klotzbach *et al.*, 2020; Klotzbach *et al.*, 2022a). We find various hurricane-centred hazard, exposure and vulnerability quantities correlate significantly with losses (i.e., $r > 0.5$), but using a weighted-rank-sum approach to optimally combine these predictors yields markedly more skilful loss predictions ($\rho = 0.89$ for all storms). This high correlation between loss observations and predictions, with a significantly reduced RMSE of U.S.$ 7.0 bn, improves the predicted loss rank of the most impactful historical cases. This optimal prediction model was derived by determining the weighted sum of normalised ranks of landfall c_p, maximum rainfall accumulation, and the percentage of total GHSL building density damage within R64 and within 12 hours of landfall. This model includes two hazard attributes representing hurricane intensity (c_p and rainfall), building density impacted, and applies a vulnerability function (percentage of building damage proportional to v_{max}). For this model, important limitations are related to the observational uncertainties within the input predictor data, as well as in the target variable. There is significant variance among loss estimates for historical events. Additional uncertainty stems from the lack of complete cyclone size information prior to 2002, which is not completely mitigated by our statistical estimation approach and could impact skill for pre-2002 landfalls. A key data gap is the availability of vulnerability information and its temporal granularity. Lastly, historical loss uncertainty necessitated consideration of multiple datasets and averaging losses where required.

Studies based on physical climate model outputs provide evidence of significant interannual to decadal variability in damage (Lavender *et al*., 2020) and substantial inter-model uncertainty (Meiler *et al*., 2023). Projected increases in vulnerable assets, assuming no adaptation, may worsen damage to a greater extent than physical hazard changes (Gettelman *et al*., 2017). Regional vulnerability, particularly building characteristics, is important, and regional factors are accounted for in high-resolution catastrophe models (e.g., Eberenz *et al*. 2021) and synthetic tropical cyclone models (e.g., Meiler *et al*., 2022), although results exhibit sensitivity to model setup (Meiler *et al*., 2025). Open-source catastrophe models may underestimate historical losses (König, 2017; Welker *et al*., 2021), so a comprehensive intercomparison of such models across historical

hurricanes is warranted. While our statistical model may not predict hurricane losses events outside our sample (i.e., loss significantly exceeding that of Hurricane Katrina), it ranks losses in historical context and complements other catastrophe modelling approaches.

7.1.2 A loss-based hurricane scale effectively communicates economic impacts

We devised a 'Hurricane Predictive Loss Scale' in which hurricanes are assigned a 'loss category'. This aids characterising historical hurricanes according to economic losses, complementing the Saffir–Simpson scale and prior work (Bloemendaal *et al.*, 2021; Pilkington and Mahmoud, 2016). Our model-predicted 'loss categories' matched observed categories (determined from loss data) in 70% of cases, comparing favourably with the Saffir–Simpson scale. An illustrative example is Hurricane Sandy (2012), a lower-intensity, larger-size storm that is assigned 'loss category 4', a more appropriate characterisation of the actual loss. The HPLS offers a simple method to embed information about potential losses for forecast landfalls to support decision-making. In (re-)insurance, pooling risk across a diversified portfolio reduces capital costs and increases loss predictability (Ciullo *et al*., 2023). For hurricanes, however, recent basin-wide (e.g., Klotzbach *et al*., 2022) and near-coast (e.g., Qi *et al*., 2025; Wang *et al*., 2021; Zhong *et al*., 2026) trends in hazards will increasingly challenge risk stakeholders. We therefore anticipate that our scheme will be a useful risk-management tool.

7.2. Outlook

Our study highlights clear data needs. First, vulnerability data of higher spatial and, in particular, temporal granularity are needed. Using open-source datasets here necessitated a combination of time-varying and time-invariant predictors, which is an area for improvement. The development of such datasets using emerging technologies offers potential—for example, combining machine learning and satellite imagery to describe building attributes and structural vulnerability, and their changes, with higher fidelity. Vulnerability may be economic or social and characterised by economic or demographic data, respectively (Wilson *et al*., 2022). Second, there is a need for hurricane size information for historical events. This key physical quantity directly determines impacted areas (Wang and Toumi, 2016), and future work to reconstruct wind radii would be considerably beneficial. It is somewhat unclear how climate change may impact the horizontal structure of a hurricane's wind field. Expansion rates increase with sea-surface warming (Wang *et al*., 2025), yet outer size is not projected to change over this

485 century (Schenkel *et al.*, 2023). Studies of high-resolution climate models, which adequately capture intensification and
486 horizontal structure (Baker *et al*., 2024), may help substantiate projections and evaluate their risk implications.

487 There is potential to refine our approach for application to a variety of sectors and stakeholders (Beven *et al*., 2018). We
488 developed a loss-based classification, but different schemes could be developed for specific sectors. For example,
489 governments, disaster-relief organisations and public-health services may employ classification based on expected fatalities,
490 requiring an understanding of human factors, such as risk perception (Wong-Parodi and Garfin, 2022) and the ability of
491 communities to respond to warnings (Black *et al*., 2013). Predictions of human impacts could be made following our statistical
492 framework, given adequate historical mortality-burden data. Additionally, our methodology may be applied to other cyclone-
493 prone regions, where necessary data are available. Finally, our predictive model may help quantify hurricane risk changes in
494 a warming climate by application to simulated future hurricanes, which may be more intense and induce heavier precipitation
495 (Knutson *et al.*, 2020), to quantify how losses may respond to hazard changes and the expected losses due to unprecedented
496 landfalls in regions of significant exposure or vulnerability.

497

498 **8 Acknowledgements**

499

500 AJB is supported by the National Centre for Atmospheric Science and by the nextGEMS (European Union Horizon2020 grant
501 agreement 101003470) and Huracán (NERC–NSF grant agreement NE/W009587/1) projects. Data analysis in this study was
502 facilitated by JASMIN (jasmin.ac.uk), which is operated by the Science and Technology Facilities Council on behalf of the
503 Natural Environment Research Council.

504

505

506 **9 Author contributions**

507

508 AFV and AJB conceived the study. AFV performed data analysis and figure preparation, supported by AJB, VMH and JM.
509 AFV and AJB wrote the manuscript. All authors interpreted results and approved the final draft.

510

511

512 **10 Competing interests**

513

514 The authors declare no competing interests.

515

516

11 Code / data availability

IBTrACS data are available from ncei.noaa.gov/products/international-best-track-archive. All other datasets are available from the cited sources. Data analysis and visualisation code is available at github.com/ncas-metoffice-hrcm/hurricane_loss.

References

AON, 2025. 2025 Climate and Catastrophe Insight. Available: https://www.aon.com/en/insights/reports/climate-and-catastrophe-report [Accessed 16 Sept 2025].

Aznar-Siguan, G., & Bresch, D. N. (2019). CLIMADA v1: A global weather and climate risk assessment platform. *Geoscientific Model Development* **12**, 3085–3097.

Baker, A. J., Vannière, B., and Vidale, P. L., 2024. On the realism of tropical cyclones simulated in global storm-resolving climate models. *Geophysical Research Letters* **51**, e2024GL109841 (2024).

Baldwin, J. W., Lee, C.-Y., Walsh, B. J., Camargo, S. J. and Sobel, A. H., 2023. Vulnerability in a Tropical Cyclone Risk Model: Philippines Case Study. *Weather, Climate, and Society* **15**, 503-523.

Beck, H. E., Wood, E. F., Pan, M., Fisher, C. K., Miralles, D. G., van Dijk, A. I. J. M., McVicar, T. R. and Adler, R. F., 2019. MSWEP V2 Global 3-Hourly 0.1° Precipitation: Methodology and Quantitative Assessment. *Bulletin of the American Meteorological Society* **100**, 473-500.

Berlemann, M. & Wenzel, D. Hurricanes, economic growth and transmission channels: Empirical evidence for countries on differing levels of development. *World Development* **105**, 231–247 (2018).

Beven, K. J., Almeida, S., Aspinall, W. P., Bates, P. D., Blazkova, S., Borgomeo, E., Freer, J., Goda, K., Hall, J. W., Phillips, J. C., Simpson, M., Smith, P. J., Stephenson, D. B., Wagener, T., Watson, M. & Wilkins, K. L. Epistemic uncertainties and natural hazard risk assessment – Part 1: A review of different natural hazard areas. *Nat. Hazards Earth Syst. Sci.* **18**, 2741–2768 (2018).

Black, R., Arnell, N. W., Adger, W. N., Thomas, D. & Geddes, A. Migration, immobility and displacement outcomes following extreme events. *Environmental Science & Policy* **27**, S32–S43 (2013).

Blake, E. S., Landsea, C. and Gibney, E. J. 2011. The deadliest, costliest, and most intense United States tropical cyclones from 1851 to 2010 (and other frequently requested hurricane facts). NOAA technical memorandum NWS NHC-6.

Bloemendaal, N., de Moel, H., Mol, J. M., Bosma, P. R. M., Polen, A. N. and Collins, J. M., 2021. Adequately reflecting the severity of tropical cyclones using the new Tropical Cyclone Severity Scale. *Environmental Research Letters* **16**, 014048.

Cass, E., W. Shao, F. Hao, H. Moradkhani, and E. Yeates, 2023: Identifying trends in interpretation and responses to hurricane and climate change communication tools. *International Journal of Disaster Risk Reduction* **93**, 103752.

Camelo, J. and Mayo, T., 2021. The lasting impacts of the Saffir-Simpson Hurricane Wind Scale on storm surge risk communication: The need for multidisciplinary research in addressing a multidisciplinary challenge. *Weather and Climate Extremes* **33**, 100335.

Chavas, D. R., Knaff, J. A. and Klotzbach, P., 2025. A Simple Model for Predicting Tropical Cyclone Minimum Central Pressure from Intensity and Size. *Weather and Forecasting* **40**, 333-346.

Chavas, D. R., Lin, N. and Emanuel, K., 2015. A Model for the Complete Radial Structure of the Tropical Cyclone Wind Field. Part I: Comparison with Observed Structure. *Journal of the Atmospheric Sciences* **72**, 3647-3662.

Chavas, D. R., Reed, K. A. and Knaff, J. A., 2017. Physical understanding of the tropical cyclone wind-pressure relationship. *Nature Communications* **8**, 1360.

Ciullo, A., Strobl, E., Meiler, S., Martius, O. & Bresch, D. N. Increasing countries' financial resilience through global catastrophe risk pooling. *Nature Communications* **14**, 922 (2023).

Copernicus Climate Change Service (2022): Global sea level change time series from 1950 to 2050 derived from reanalysis and high resolution CMIP6 climate projections. Copernicus Climate Change Service (C3S) Climate Data Store (CDS). DOI: 10.24381/cds.a6d42d60 [Accessed 18 May 2025].

Delforge, D., Wathelet, V., Below, R., Sofia, C. L., Tonnelier, M., van Loenhout, J. A. F. and Speybroeck, N., 2025. EM-DAT: the Emergency Events Database. *International Journal of Disaster Risk Reduction* **124**, 105509.

Eberenz, S., Stocker, D., Röösli, T. and Bresch, D. N., 2020. Asset exposure data for global physical risk assessment. *Earth System Science Data* **12**, 817-833.

Emanuel, K., 2011. Global Warming Effects on U.S. Hurricane Damage. *Weather, Climate, and Society* **3**, 261-268.

Federal Emergency Management Agency, 2024a. *Hazus Hurricane Model Technical Manual, Hazus 6.1*. https://www.fema.gov/sites/default/files/documents/Hazus_6.1_Hurricane_Model_Technical_Manual.pdf [Accessed 18 May 2025].

Federal Emergency Management Agency, 2024b. National Risk Index: Future Risk Technical Documentation. Available: https://eelp.law.harvard.edu/wp-content/uploads/2025/03/NRI_Future_Risk_Technical_Document.pdf [Accessed 18 May 2025].

Federal Emergency Management Agency, 2025. Building Code Adoption Tracking. Available: https://www.fema.gov/emergency-managers/risk-management/building-science/bcat [Accessed 18 May 2025].

Gahtan, J., Knapp, K., Schreck III, C., Diamond, H., Kossin, J. and Kruk, M. C. 2024. International Best Track Archive for Climate Stewardship (IBTrACS), version 4r01. National Oceanographic and Atmospheric Administration National Centers for Environmental Information.

Gallagher Re. 2025. Gallagher Re Natural Catastrophe and Climate Report 2024. Available: https://www.ajg.com/gallagherre/-/media/files/gallagher/gallagherre/news-and-insights/2025/natural-catastrophe-and-climate-report-2025.pdf [Accessed 18 May 2025].

Gettelman, A., Bresch, D. N., Chen, C. C., Truesdale, J. E. & Bacmeister, J. T. Projections of future tropical cyclone damage with a high-resolution global climate model. *Climatic Change* **146**, 575–585 (2018).

Gori, A., Lin, N., Schenkel, B. and Chavas, D., 2023. North Atlantic Tropical Cyclone Size and Storm Surge Reconstructions From 1950-Present. *Journal of Geophysical Research: Atmospheres* **128**, e2022JD037312.

Gori, A., Lin, N., Chavas, D., Oppenheimer, M. & Xian, S. Sensitivity of tropical cyclone risk across the US to changes in storm climatology and socioeconomic growth. *Environmental Research Letters* **20**, 064050 (2025).

Grinsted, A., Ditlevsen, P. and Christensen, J. H., 2019. Normalized US hurricane damage estimates using area of total destruction, 1900−2018. *Proceedings of the National Academy of Sciences*, 201912277.

Hersbach, H., Bell, B., Berrisford, P., Hirahara, S., Horányi, A., Muñoz-Sabater, J., Nicolas, J., Peubey, C., Radu, R., Schepers, D., Simmons, A., Soci, C., Abdalla, S., Abellan, X., Balsamo, G., Bechtold, P., Biavati, G., Bidlot, J., Bonavita, M., De Chiara, G., Dahlgren, P., Dee, D., Diamantakis, M., Dragani, R., Flemming, J., Forbes, R., Fuentes, M., Geer, A., Haimberger, L., Healy, S., Hogan, R. J., Hólm, E., Janisková, M., Keeley, S., Laloyaux, P., Lopez, P., Lupu, C., Radnoti, G., de Rosnay, P., Rozum, I., Vamborg, F., Villaume, S. and Thépaut, J.-N., 2020. The ERA5 global reanalysis. *Quarterly Journal of the Royal Meteorological Society* **146**, 1999-2049.

Hsiang, S. M., and A. S. Jina, 2014: The causal effect of environmental catastrophe on long-run economic growth: evidence from 6,700 cyclones. NBER Working Paper No. 20352, National Bureau of Economic Research.

Holland, G. J., Belanger, J. I., & Fritz, A. (2010). A revised model for radial profiles of hurricane winds. *Monthly Weather Review,* **138**(12), 4393–4401.

Hurricane Research Division. 2025. Detailed List of Continental United States Hurricane Impacts/Landfalls. Available: http://www.aoml.noaa.gov/hrd/hurdat/UShurrs_detailed.html [Accessed 18 May 2025].

Ibrahim, H.A., Elawady, A. and Prevatt, D.O., 2024. Empirical hurricane fragility assessment of elevated and slab-on-grade residential houses. International Journal of Disaster Risk Reduction, 110, p.104663.

Intergovernmental Panel on Climate Change 2012. Managing the Risks of Extreme Events and Disasters to Advance Climate Change Adaptation. A Special Report of Working Groups I and II of the Intergovernmental Panel on Climate Change. *In:* Field, C. B., V. Barros, T. F. Stocker, D. Qin, D. J. Dokken, K. L. Ebi, M. D. Mastrandrea, K. J. Mach, G.-K. Plattner, S. K. Allen, M. Tignor, and P. M. Midgley. (ed.). Cambridge University Press, Cambridge, UK, and New York, NY, USA.

Jewson, S., 2023. The Impact of Projected Changes in Hurricane Frequencies on U.S. Hurricane Wind and Surge Damage. *Journal of Applied Meteorology and Climatology* **62**, 1827-1843.

Kelman, I., 2013: Saffir–Simpson Hurricane Intensity Scale. *Encyclopedia of Natural Hazards*, P. T. Bobrowsky, Ed., Springer, Dordrecht.

Kernkamp, H. W. J., Van Dam, A., Stelling, G. S. & de Goede, E. D. Efficient scheme for the shallow water equations on unstructured grids with application to the Continental Shelf. *Ocean Dynamics* **61**, 1175–1188 (2011).

Klotzbach, P. J., Bell, M. M., Bowen, S. G., Gibney, E. J., Knapp, K. R. and Schreck III, C. J., 2020. Surface Pressure a More Skillful Predictor of Normalized Hurricane Damage than Maximum Sustained Wind. *Bulletin of the American Meteorological Society* **101**, E830-E846.

Klotzbach, P. J., Chavas, D. R., Bell, M. M., Bowen, S. G., Gibney, E. J. and Schreck III, C. J., 2022a. Characterizing Continental US Hurricane Risk: Which Intensity Metric Is Best? *Journal of Geophysical Research: Atmospheres* **127**, e2022JD037030.

Klotzbach, P. J., Wood, K. M., Schreck III, C. J., Bowen, S. G., Patricola, C. M. and Bell, M. M., 2022b. Trends in Global Tropical Cyclone Activity: 1990–2021. *Geophysical Research Letters* **49**, e2021GL095774.

Knutson, T., Camargo, S. J., Chan, J. C. L., Emanuel, K., Ho, C.-H., Kossin, J., Mohapatra, M., Satoh, M., Sugi, M., Walsh, K. and Wu, L., 2020. Tropical Cyclones and Climate Change Assessment: Part II: Projected Response to Anthropogenic Warming. *Bulletin of the American Meteorological Society* **101**, E303-E322.

Landsea, C. W. and Franklin, J. L., 2013. Atlantic Hurricane Database Uncertainty and Presentation of a New Database Format. *Monthly Weather Review* **141**, 3576-3592.

Lavender, S. L., Walsh, K. J. E., Utembe, S., Caron, L.-P. & Guishard, M. Estimation of maximum seasonal tropical cyclone damage in the Atlantic using climate models. *Natural Hazards* **110**, 1025–1038 (2022).

Lockwood, J. F., Dunstone, N., Hermanson, L., Saville, G. R., Scaife, A. A., Smith, D. and Thornton, H. E., 2023. A Decadal Climate Service for Insurance: Skillful Multiyear Predictions of North Atlantic Hurricane Activity and U.S. Hurricane Damage. *Journal of Applied Meteorology and Climatology* **62**, 1151-1163.

Meiler, S., Vogt, T., Bloemendaal, N., Ciullo, A., Lee, C.-Y., Camargo, S. J., Emanuel, K. & Bresch, D. N. Intercomparison of regional loss estimates from global synthetic tropical cyclone models. *Nature Communications* **13**, 6156 (2022).

Meiler, S., Ciullo, A., Kropf, C. M., Emanuel, K. & Bresch, D. N. Uncertainties and sensitivities in the quantification of future tropical cyclone risk. *Communications Earth & Environment* **4**, 371 (2023).

Meiler, S., Kropf, C. M., McCaughey, J. W., Lee, C.-Y., Camargo, S. J., Sobel, A. H., Bloemendaal, N., Emanuel, K. & Bresch, D. N. Navigating and attributing uncertainty in future tropical cyclone risk estimates. *Science Advances* **11**, eadn4607 (2025).

Muller, J., Mooney, K., Bowen, S. G., Klotzbach, P. J., Martin, T., Philp, T. J., Dhruvkumar, B., Dixon, R. S. and Girimurugan, S. B., 2025. Normalized Hurricane Damage in the United States: 1900–2022. *Bulletin of the American Meteorological Society* **106**, E51-E67.

National Centers for Environmental Information, 2021. The Saffir-Simpson Hurricane Wind Scale. Available: https://www.nhc.noaa.gov/pdf/sshws.pdf [Accessed 18 May 2025].

National Centers for Environmental Information, 2025. U.S. Billion-Dollar Weather and Climate Disasters. Available: https://www.ncei.noaa.gov/access/billions/ [Accessed 18 May 2025].

National Oceanographic and Atmospheric Administration, 2024. Hurricane Costs. Available: https://coast.noaa.gov/states/fast-facts/hurricane-costs.html [Accessed 18 May 2025].

National Oceanographic and Atmospheric Administration, 2025. Tropical Cyclone Rainfall. Available: https://www.wpc.ncep.noaa.gov/tropical/rain/tcrainfall.html [Accessed 18 May 2025].

Oasis Loss Modelling Framework, (2025). *Oasis Loss Modelling Framework* (Oasis LMF) [open-source catastrophe modelling platform]. https://oasislmf.org

Oliver-Smith, A., 2020. Hurricanes, Climate Change, and the Social Construction of Risk. *International Journal of Mass Emergencies & Disasters* **38**, 1-12.

Pesaresi, M. and Politis, P. 2023. GHS-BUILT-S R2023A – GHS built-up surface grid, derived from Sentinel2 composite and Landsat, multitemporal (1975–2030). European Commission, Joint Research Centre.

Pilkington, S. F. and Mahmoud, H. N., 2016. Using artificial neural networks to forecast economic impact of multi-hazard hurricane-based events. *Sustainable and Resilient Infrastructure* **1**, 63-83.

Qi, W., Yong, B., Ritchie, E. A., Tyo, J. S. & Toumi, R. Global Increase of Tropical Cyclone Precipitation Rate Toward Coasts. *Geophysical Research Letters* **52**, e2025GL115500 (2025).

Rappaport, E. N., 2014. Fatalities in the United States from Atlantic Tropical Cyclones: New Data and Interpretation. *Bulletin of the American Meteorological Society* **95**, 341-346.

Schenkel, B. A., Chavas, D., Lin, N., Knutson, T., Vecchi, G. and Brammer, A., 2023. North Atlantic Tropical Cyclone Outer Size and Structure Remain Unchanged by the Late Twenty-First Century. *Journal of Climate* **36**, 359-382.

Stansfield, A. M., Reed, K. A., Zarzycki, C. M., Ullrich, P. A. & Chavas, D. R. Assessing Tropical Cyclones' Contribution to Precipitation over the Eastern United States and Sensitivity to the Variable-Resolution Domain Extent. *Journal of Hydrometeorology* **21**, 1425–1445 (2020).

Stansfield, A. M. & Reed, K. A. Global tropical cyclone precipitation scaling with sea surface temperature. *npj Climate and Atmospheric Science* **6**, 60 (2023).

Tripathy, S. S., K. Jafarzadegan, H. Moftakhari, and H. Moradkhani, 2024: Dynamic bivariate hazard forecasting of hurricanes for improved disaster preparedness. Communications Earth & Environment, **5**, 12.

U.S. Bureau of Economic Analysis, 2023. Current-cost net stock of fixed assets and consumer durable goods [K1WTOTL1ES000]. Available: https://fred.stlouisfed.org/series/K1WTOTL1ES000 [Accessed 18 May 2025].

U.S. Bureau of Economic Analysis, 2025. National Data Fixed Assets Accounts Tables. Available: https://apps.bea.gov/iTable/?reqid=10&step=3&isuri=1&table_list=16 [Accessed 18 May 2025].

U.S. Census Bureau, 2024. American Community Survey Housing Units by Year Built Variables — Tract. Available: https://hub.scag.ca.gov/datasets/41c90eef3a12451faff10c2a6b26fc46_2/about [Accessed 18 May 2025].

Vickery, P., J., Skerlj, P., F., Lin, J., Twisdale, L., A., Young, M., A. and Lavelle, F., M., 2006. HAZUS-MH Hurricane Model Methodology. II: Damage and Loss Estimation. *Natural Hazards Review* **7**, 94-103.

Wang, X., Verlaan, M., Apecechea, M. I. & Lin, H. X. Computation-Efficient Parameter Estimation for a High-Resolution Global Tide and Surge Model. *Journal of Geophysical Research: Oceans* **126**, e2020JC016917 (2021).

Wang, S. & Toumi, R. On the relationship between hurricane cost and the integrated wind profile. *Environmental Research Letters* **11**, 114005 (2016).Wang, S. & Toumi, R. Recent migration of tropical cyclones toward coasts. *Science* **371**, 514 (2021).

Wang, D., Chavas, D. R. & Schenkel, B. A. Tropical cyclones expand faster at warmer relative sea surface temperature. *Proceedings of the National Academy of Sciences* **122**, e2424385122 (2025).

Ward, P. J., Blauhut, V., Bloemendaal, N., Daniell, J. E., de Ruiter, M. C., Duncan, M. J., Emberson, R., Jenkins, S. F., Kirschbaum, D., Kunz, M., Mohr, S., Muis, S., Riddell, G. A., Schäfer, A., Stanley, T., Veldkamp, T. I. E. and Winsemius, H. C., 2020. Natural hazard risk assessments at the global scale. *Nat. Hazards Earth Syst. Sci.* **20**, 1069-1096.

Wehner, M. F. and Kossin, J. P., 2024. The growing inadequacy of an open-ended Saffir–Simpson hurricane wind scale in a warming world. *Proceedings of the National Academy of Sciences* **121**, e2308901121.

Weinkle, J., Landsea, C., Collins, D., Musulin, R., Crompton, R. P., Klotzbach, P. J. and Pielke, R., 2018. Normalized hurricane damage in the continental United States 1900–2017. *Nature Sustainability* **1**, 808-813.

Willis Towers Watson. 2024. Natural Catastrophe Review 2024. Available: https://www.wtwco.com/en-eg/insights/2025/01/wtw-natural-catastrophe-review-2024 [Accessed 18 May 2025].

Wilson, K. M., J. W. Baldwin, and R. M. Young, 2022: Estimating Tropical Cyclone Vulnerability: A Review of Different Open-Source Approaches. Hurricane Risk in a Changing Climate, J. M. Collins, and J. M. Done, Eds., Springer International Publishing, 255–281.

Wong-Parodi, G. & Garfin, D. R. Hurricane adaptation behaviors in Texas and Florida: exploring the roles of negative personal experience and subjective attribution to climate change. *Environmental Research Letters* **17**, 034033 (2022).

WorldPop 2018. Global High Resolution Population Denominators Project. www.worldpop.org — School of Geography and Environmental Science, University of Southampton. Funded by The Bill and Melinda Gates Foundation (OPP1134076).

Young, R. and Hsiang, S., 2024. Mortality caused by tropical cyclones in the United States. *Nature* **635**, 121-128.

Zhong, Q., Gan, J., Tu, S., Toumi, R. & Chan, J. C. L. Global increase in rain rate of tropical cyclones prior to landfall. *Nature Communications* **17**, 114 (2026).

Zuzak, C., Goodenough, E., Stanton, C., Mowrer, M., Ranalli, N., Kealey, D. and Rozelle, J. 2021. National risk index technical documentation, 37. Available: https://hazards.fema.gov/nri [Accessed 18 May 2025].